2E1-2

Conformal Dispersive Finite-Difference Time-Domain Simulations of Plasmonic Waveguides

Yan Zhao, and # Yang Hao
Department of Electronic Engineering, Queen Mary, University of London
Mile End Road, London E1 4NS, UK
y.hao@elec.qmul.ac.uk

1. Introduction

Recently there have been growing interests in the study and fabrication of chains of metallic nanoparticles namely plasmonic waveguides as subwavelength guiding structures due to the existence of highly localised surface plasmons [1]. In this context, the finite-difference time-domain (FDTD) method [2] is seen as the most popular numerical technique in the study of these structures especially because of its flexibility in handling material dispersion as well as arbitrary shaped inclusions. However unless using extremely fine meshes, due to the nature of orthogonal and staggered grid of conventional FDTD, often modifications need to be applied in order to improve the accuracy of modelling, such as the treatment of interfaces between different materials even for planar structures [3], and the improved conformal algorithms using structured meshes [4] for curved surfaces.

In addition to the modifications at material interfaces, the material frequency dispersion has also to be taken into account in FDTD modelling [5]. However, modelling dispersive materials with curved surfaces still remains to be a challenging topic due to the complexity in algorithm as well as the introduction of numerical instability. An alternative way to solve this problem is based on the idea of effective permittivities (EPs) [6] in the underlying Cartesian coordinate system, and the dispersive FDTD scheme can be therefore modified accordingly without affecting the stability of algorithm. In this paper, we propose a novel conformal dispersive FDTD algorithm combining the EPs together with an auxiliary differential equation (ADE) method [2]. Numerical FDTD simulation results are verified by a frequency domain embedding method [7].

2. Conformal Dispersive FDTD Method using Effective Permittivity

There are many types of EPs in literature [6, 8, 9], in this paper, we have chosen the most recently reported one [9] to develop the conformal dispersive FDTD method. The conformal dispersive FDTD method using other EPs can be developed in a similar manner. According to [9], the EP in a general form is given by

$$\varepsilon_{\text{eff}} = \varepsilon_{\parallel}(1 - n^2) + \varepsilon_{\perp} n^2, \tag{1}$$

where n is the projection of the unit normal vector $\mathbf{n}$ along the field component as shown in Fig. 1(a), $\varepsilon_{\parallel}$ and $\varepsilon_{\perp}$ are parallel and perpendicular permittivities to the material interface, respectively and defined as

$$\varepsilon_{\parallel} = f\varepsilon_2 + (1 - f)\varepsilon_1, \qquad \varepsilon_{\perp} = [f/\varepsilon_2 + (1 - f)/\varepsilon_1]^{-1}, \tag{2}$$

where f is the filling ratio of material ε_2 in a certain FDTD cell. Figure 1(b)(top) shows an example layout of an infinite-long cylinder in the free space represented using staircase approximations in a two-dimensional (2-D) orthogonal FDTD domain. The approximated shape introduces spurious numerical resonant modes which do not exist in actual structures. On the other hand, using the concept of filling ratio, the curvature can be properly represented in FDTD domain as shown in Fig. 1(b)(bottom), where different levels of darkness indicate different filling ratios of material ε_2. The accuracy of modelling can be significantly improved compared with staircase approximations, as will be shown in a later section.

ISBN: 978-4-88552-223-9 C3055

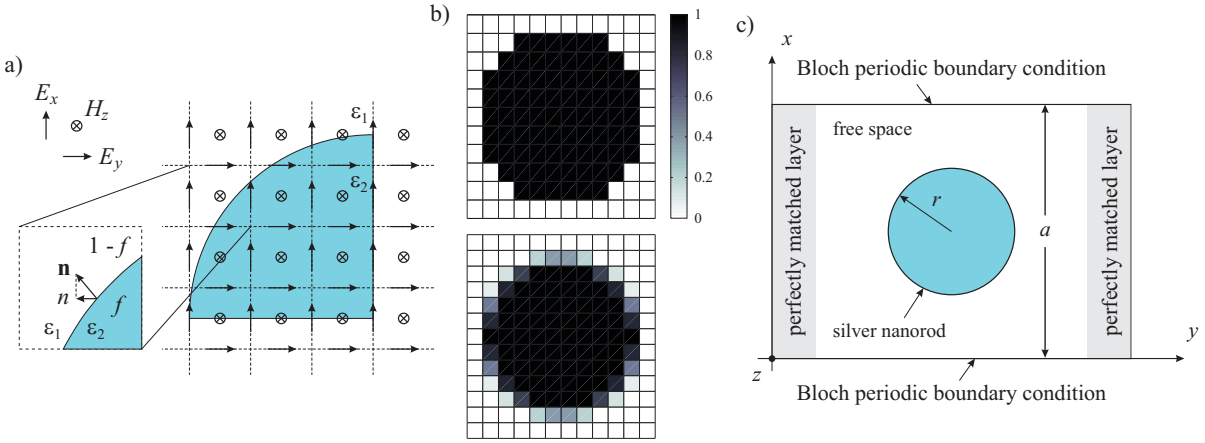

Fig. 1. (a) Layout of a quarter circular inclusion in orthogonal FDTD grid for E_y component for an example of the radius of inclusion is three FDTD cells. (b) Comparison of the filling ratio for E_y component using staircase approximations (top) and the conformal scheme (bottom). The radius of circular cylinder is five cells. (c) Two-dimensional (2-D) FDTD simulation domain for calculation of dispersion diagram.

In this paper we consider silver cylinders as the inclusions, which at optical frequencies can be modelled using the Drude dispersion model

$$\varepsilon_2 = 1 - \frac{\omega_p^2}{\omega^2 - j\omega\gamma}, \tag{3}$$

where ω_p is the plasma frequency and γ is the collision frequency. In this paper, we assume that the silver cylinders are embedded in the free space ($\varepsilon_1 = 1$). Substitute (2) into (1) and apply inverse Fourier transformation i.e. $j\omega \rightarrow \partial/\partial t$, after simple calculations we obtain the constitutive relation in the time domain as

$$\begin{aligned} &\frac{\partial^4 \mathbf{D}}{\partial t^4} + 2\gamma\frac{\partial^3 \mathbf{D}}{\partial t^3} + [\gamma^2 + (1-f)\omega_p^2]\frac{\partial^2 \mathbf{D}}{\partial t^2} + \gamma(1-f)\omega_p^2\frac{\partial \mathbf{D}}{\partial t} \\ &= \frac{\partial^4 \mathbf{E}}{\partial t^4} + 2\gamma\frac{\partial^3 \mathbf{E}}{\partial t^3} + (\gamma^2 + \omega_p^2)\frac{\partial^2 \mathbf{E}}{\partial t^2} + \gamma\omega_p^2\frac{\partial \mathbf{E}}{\partial t} + f(1-f)(1-n^2)\omega_p^4\mathbf{E}. \end{aligned} \tag{4}$$

Following standard discretisation procedure using central finite difference approximations [2], the updating equation for $\mathbf{E}$ in FDTD iterations is obtained as

$$\mathbf{E}^{n+1} = a_0^{-1}[b_0\mathbf{D}^{n+1} + b_1\mathbf{D}^n + b_2\mathbf{D}^{n-1} + b_3\mathbf{D}^{n-2} + b_4\mathbf{D}^{n-3} - (a_1\mathbf{E}^n + a_2\mathbf{E}^{n-1} + a_3\mathbf{E}^{n-2} + a_4\mathbf{E}^{n-3})], \tag{5}$$

with the coefficients given by

$$\begin{aligned}
a_0 &= \frac{1}{(\Delta t)^4} + \frac{\gamma}{(\Delta t)^3} + \frac{\gamma^2+\omega_p^2}{4(\Delta t)^2} + \frac{\gamma\omega_p^2}{8\Delta t} + \frac{f(1-f)(1-n^2)\omega_p^4}{16}, & b_0 &= \frac{1}{(\Delta t)^4} + \frac{\gamma}{(\Delta t)^3} + \frac{\gamma^2+(1-f)\omega_p^2}{4(\Delta t)^2} + \frac{\gamma(1-f)\omega_p^2}{8\Delta t}, \\
a_1 &= -\frac{4}{(\Delta t)^4} - \frac{2\gamma}{(\Delta t)^3} + \frac{\gamma\omega_p^2}{4\Delta t} + \frac{f(1-f)(1-n^2)\omega_p^4}{4}, & b_1 &= -\frac{4}{(\Delta t)^4} - \frac{2\gamma}{(\Delta t)^3} + \frac{\gamma(1-f)\omega_p^2}{4\Delta t}, \\
a_2 &= \frac{6}{(\Delta t)^4} - \frac{\gamma^2+\omega_p^2}{2(\Delta t)^2} + \frac{3f(1-f)(1-n^2)\omega_p^4}{8}, & b_2 &= \frac{6}{(\Delta t)^4} - \frac{\gamma^2+(1-f)\omega_p^2}{2(\Delta t)^2}, \\
a_3 &= -\frac{4}{(\Delta t)^4} + \frac{2\gamma}{(\Delta t)^3} - \frac{\gamma\omega_p^2}{4\Delta t} + \frac{f(1-f)(1-n^2)\omega_p^4}{4}, & b_3 &= -\frac{4}{(\Delta t)^4} + \frac{2\gamma}{(\Delta t)^3} - \frac{\gamma(1-f)\omega_p^2}{4\Delta t}, \\
a_4 &= \frac{1}{(\Delta t)^4} - \frac{\gamma}{(\Delta t)^3} + \frac{\gamma^2+\omega_p^2}{4(\Delta t)^2} - \frac{\gamma\omega_p^2}{8\Delta t} + \frac{f(1-f)(1-n^2)\omega_p^4}{16}, & b_4 &= \frac{1}{(\Delta t)^4} - \frac{\gamma}{(\Delta t)^3} + \frac{\gamma^2+(1-f)\omega_p^2}{4(\Delta t)^2} - \frac{\gamma(1-f)\omega_p^2}{8\Delta t},
\end{aligned}$$

The computations of $\mathbf{H}$ and $\mathbf{D}$ are performed using Yee's standard updating equations in the free space.

3. Numerical Tests

In our simulations, we have used the developed conformal dispersive FDTD method to calculate the dispersion diagram for one-dimensional (1-D) plasmonic waveguide formed by an array of periodic

circular infinite-long (along z-direction) silver cylinders. As shown in Fig. 1(c), the 2-D simulation domain with TE polarisation is truncated using Bloch's periodic boundary conditions (PBCs) [10] in x-direction and Berenger's perfectly matched layers (PMLs) [11] along y-direction. The radius of silver cylinders is $r = 2.5\times10^{-8}$ m and the period is $a = 7.5\times10^{-8}$ m. The plasma and collision frequencies are $\omega_p = 9.39\times10^{15}$ rad/s and $\gamma = 3.14\times10^{13}$ Hz, respectively. The FDTD cell size is $\Delta x = \Delta y = 2.5\times10^{-9}$ m with the time step $\Delta t = \Delta x/\sqrt{2}c$ s according to the Courant stability criterion [2]. A wideband magnetic line source is placed at a random location in the free space region of the 2-D simulation domain in order to excite all resonant modes of the structure. The magnetic fields at one hundred random locations in the free space region are recorded during simulations, transformed into the frequency domain and combined to extract individual resonant mode corresponding to each local maximum. For each wave vector, a total number of 20,000 time steps are used in our simulations to obtain enough accurate frequency domain results.

In order to demonstrate the advantage of the EP in dispersive FDTD calculations, we have also performed simulations using staircase approximations for the circular cylinder. Figure 2(a) shows the comparison of the first resonant mode (transverse mode) of the plasmonic waveguide calculated using different methods. With the same FDTD spatial resolution, the model using EP shows excellent agree-

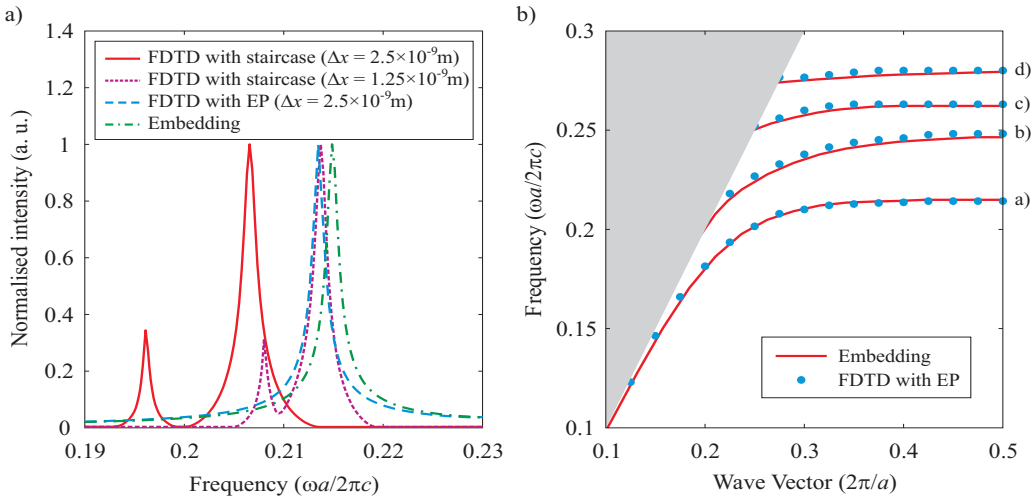

Fig. 2. (a) Comparison of the first resonant frequency (transverse mode) at wave vector $k_x = \pi/a$ calculated using the FDTD method with staircase approximations, the FDTD method with EPs and the frequency domain embedding method. (b) Comparison of dispersion diagrams calculated using the FDTD method with EPs and the frequency domain embedding method.

ment with the results from the frequency domain embedding method [7], on the contrary, the staircase approximation not only leads to a shift of the main resonant frequency, but also introduces a spurious numerical resonant mode which does not exist in actual structures. The same effect has also been found for non-dispersive dielectric cylinders [12]. It is also shown in Fig. 2(a) that although one may correct the main resonant frequency using finer meshes, the spurious resonant mode still remains.

The problem of frequency shift and spurious modes become severer when calculating higher guided modes near the 'flat band' region (i.e the region where waves travel at a very low phase velocity). Even with refined spatial resolution, the staircase approximation fails to provide correct results (not shown). On the other hand, using the proposed conformal dispersive FDTD scheme, all resonant modes are correctly captured in FDTD simulations as demonstrated by the comparison with the embedding method as shown in Fig. 2(b).

For demonstration of field symmetries and due to the TE mode considered in our simulations, we have plotted the distributions of magnetic field corresponding to different resonant modes at wave number $k_x = \pi/a$ as marked in Fig. 2(b), as shown in Fig. 3. Sinusoidal sources for excitation of certain single mode are used and the sources are placed at different locations corresponding to different symmetries of field patterns. All field patterns are plotted after the steady state is reached in simulations. The modes

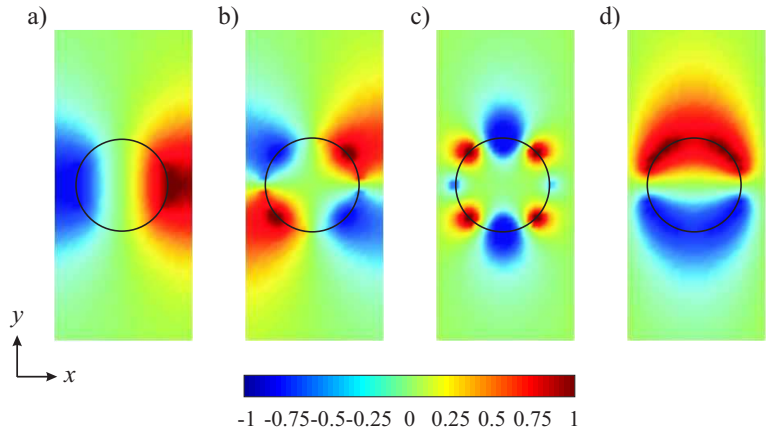

Fig. 3. Normalised distributions of magnetic field corresponding to different resonant modes at wave number $k_x = \pi/a$ as marked in Fig. 2(b): (a), (c) - even modes and (b), (d) - odd modes.

(a), (c) in Fig. 3 are even modes and (b), (d) are considered as odd modes.

4. Conclusions

We have developed a conformal auxiliary differential equation based dispersive FDTD method using effective permittivities. The calculation of dispersion diagram for plasmonic waveguide formed by an array of silver cylinders is used to validate the proposed algorithm. The comparison with staircase approximations clearly demonstrates the advantage in the accuracy of proposed method for modelling of curved nano-plasmonic structures.

References

[1] S. A. Maier, P. G. Kik, H. A. Atwater, S. Meltzer, E. Harel, B. E. Koel, and A. G. Requicha, "Local detection of electromagnetic energy transport below the diffraction limit in metal nanoparticle plasmon waveguides," *Nature Materials*, vol. 2, pp. 229, 2003.

[2] A. Taflove, *Computational Electrodynamics: The Finite Difference Time Domain Method*, 2nd ed., Norwood, MA: Artech House, 2000.

[3] K.-P. Hwang, and A. C. Cangellaris, "Effective permittivities for second-order accurate FDTD equations at dielectric interfaces," *IEEE Microwave Wirel. Compon. Lett.*, vol. 11, pp. 158-160, 2001.

[4] Y. Hao, and C. J. Railton, "Analyzing electromagnetic structures with curved boundaries on Cartesian FDTD meshes," *IEEE Trans. Microwave Theory Tech.*, vol. 46, pp. 82-88, Jan. 1998.

[5] Y. Zhao, P. Belov, and Y. Hao, "Modelling of wave propagation in wire media using spatially dispersive finite-difference time-domain method: numerical aspects," accepted, *IEEE Trans. Antennas Propagat.*, 2006.

[6] N. Kaneda, B. Houshmand, and T. Itoh, "FDTD analysis of dielectric resonators with curved surfaces," *IEEE Trans. Microwave Theory Tech.*, vol. 45, pp. 1645-1649, Sep. 1997.

[7] J. E. Inglesfield, "A method of embedding," *J. Phys. C: Solid State Phys.*, vol. 14, pp. 3795-3806, 1981.

[8] J.-Y Lee and N.-H Myung, "Locally tensor conformal FDTD method for modeling arbitrary dielectric surfaces," *Microw. Opt. Tech. Lett.*, vol. 23, pp. 245-249, Nov. 1999.

[9] A. Mohammadi, and M. Agio, "Contour-path effective permittivities for the two-dimensional finite-difference time-domain method," *Opt. Express*, vol. 13, pp. 10367-10381, 2005.

[10] C. T. Chan, Q. L. Yu, and K. M. Ho, "Order-N spectral method for electromagnetic waves," *Phys. Rev. B*, vol. 51, pp. 16635-16642, 1995.

[11] J. R. Berenger, "A perfectly matched layer for the absorption of electromagnetic waves," *J. Computat. Phys.*, vol. 114, pp. 185-200, Oct. 1994.

[12] W. Song, Y. Hao, and C. Parini, "Comparison of nonorthogonal and Yee's FDTD schemes in modelling photonic crystals," submitted to *Opt. Express*, 2006.